Chronic oligodendrogenesis and remyelination after spinal cord injury in mice and rats

Zoe C. Hesp[1], Evan Goldstein[1], Carlos Miranda[4], Brain Kaspar[3,4], Dana McTigue[2,3]

[1]Neuroscience Graduate Studies Program, The Ohio State University, Columbus, OH 43210

[2]Department of Neuroscience, The Ohio State University, Columbus, OH 43210

[3]Center for Brain and Spinal Cord Repair, The Ohio State University, Columbus, OH 43210

[4]Nationwide Children's Hospital, Columbus, OH 43205

ABSTRACT

NG2 cells robustly proliferate during the first week after spinal cord injury (SCI), a portion of which give rise to new oligodendrocytes (OLs) capable of remyelination. Our prior work showed spontaneous NG2 cell proliferation for 4 weeks post-injury (wpi); whether these later responding cells still generate OLs and remyelinate axons in the chronic injury environment, however, is unknown. Here we used two PDGFαR-reporter mouse lines and rats injected with a GFP-retrovirus to assess NG2 cell fate through 80dpi. Notably, mature OLs were generated from NG2/PDGFαR cells as late as 8-12wpi. GFP+ processes of new OL lineage cells ensheathed axons at all times examined, some of which co-localized with MBP or abutted Caspr+ profiles, suggesting functional myelination. Astrocytes in chronic tissue expressed the pro-OL differentiation and survival factors CNTF and FGF-2, and also expressed pSTAT3 through 12wpi revealing active signaling of the JAK/STAT pathway, which is induced by CNTF and related factors. Finally, genes associated with NG2 cell fate determination, such as Hes5, ID2, and ID4, were significantly altered late after injury. Collectively, these data indicate that

endogenous repair processes such as oligodendrogenesis, axon ensheathment and remyelination continue chronically after SCI, revealing that the injured spinal cord remains in a very dynamic state for 2-3 months post-injury. This previously unappreciated spontaneous reparative process may potentially be leveraged therapeutically to further enhance repair, and should be a consideration when testing agents that may inadvertently disrupt it.

INTRODUCTION

NG2 cells, also known as oligodendrocyte progenitors, give rise to myelinating oligodendrocytes (OLs) during development and in adulthood (Nishiyama et al., 2009). These cells are traditionally identified by NG2 and platelet-derived growth factor alpha receptor (PDGFαR) expression (Nishiyama et al., 1996; Richardson et al., 2011) and are the most proliferative cells of adult CNS (Horner et al., 2002; Dawson et al., 2003).

NG2 cells retain their role as progenitors after injury or demyelination (Watanabe et al., 2002; Keirstead et al., 2005; Lytle et al., 2009; Tripathi et al., 2010). This is well demonstrated in the context of spinal cord injury (SCI), which causes extensive cell death and significant cell proliferation (McTigue et al., 2001; Zai and Wrathall, 2005; Horky et al., 2006; Barnabé-Heider et al., 2010; Almad et al., 2011). OLs are lost in the first hours after SCI (Zai and Wrathall, 2005), and protracted OL apoptosis continues for 2-3 weeks post-injury (wpi), especially distal to the lesion (Crowe et al., 1997; Grossman et al., 2001). Surviving OLs are post-mitotic and cannot remyelinate axons (Keirstead and Blakemore, 1997). Thus, surviving NG2 cells are the major source for OL replacement and remyelination after SCI. Previous work demonstrated significant NG2 cell proliferation during the first 4 weeks after SCI (McTigue et al., 2001; Horky et al., 2006; Lytle et al., 2006; Rabchevsky et al., 2007). Over the first 2wpi, a portion of these

dividing NG2 cells differentiates into OLs, particularly along lesion borders (Zai & Wrathall, 2005; Horky et al., 2006; Tripathi and McTigue, 2007; Lytle & Wrathall, 2007). These new OLs likely contribute to remyelination as several classic studies have shown evidence of OL remyelination beginning around 3wpi (Gledhill et al., 1973; Harisson et al., 1975). More recent work also demonstrated OL remyelination 14 days after SCI (Sellers et al., 2009).

While acute NG2 cell responses after SCI are well documented, there is a substantial gap in the literature regarding NG2 cell behavior *chronically*. It is unknown if new OLs are generated beyond 2wpi and, if so, if they remyelinate axons. Therefore, we tested the hypothesis that protracted NG2 cell proliferation results in chronic oligodendrogenesis after SCI. As lesions evolve differently between rodent models, two different PDGFαR-reporter mice lines and adult rats injected with a GFP-expressing retrovirus were used to track NG2 cell fate for 12wpi. Gene changes associated with NG2 cell fate were also examined. Results reveal that oligodendrogenesis occurs continuously for at least 8-12 wpi after spinal contusion, along with signs of functional remyelination by late-born OLs. Astrocytes in the chronic lesion environment express pro-survival growth factors for OLs and NG2 cells, and NG2 cell fate genes display dynamic changes for several weeks post-injury. Collectively these data highlight that endogenous cell replacement continues for at least 3 months after SCI and that the chronic lesion milieu remains in a dynamic state. This long-term endogenous repair should be considered when designing drug treatments or cell transplantation strategies that may either take advantage of or inadvertently disrupt this chronic spontaneous repair.

METHODS:

Spinal cord injury

All surgical and postoperative care procedures were performed in accordance with The Ohio State University Institutional Animal Care and Use Committee. Adult male and female mice (~12 weeks old) and adult female Sprague-Dawley rats (~250g) were anesthetized with a ketamine/xylazine cocktail (10mg/kg, 80mg/kg, respectively) and the spinal cord exposed at the T9 (mouse) or T8 (rat) vertebral level via a single-level laminectomy. The animals then received either a moderate-severe (75 kDyne force; mouse) or moderate (150 kDyne force; rat) spinal contusion injury using the Infinite Horizons device (Precision Instruments). A subset of rats received a comparable moderate injury with the Ohio State University electromechanic spinal cord injury device (0.9mm displacement). The muscles overlying the spinal cord were then sutured and the skin was closed using surgical clips. Animals were given 2cc (mouse) or 5cc (rat) of saline and placed in warm recovery cages. Post-surgical care included 5 days treatment with antibiotics (Gentomicin, 5 mg/kg) and saline to maintain hydration, and twice-a-day manual bladder expression until spontaneous voiding returned. Sham animals received a laminectomy as described above but did not receive spinal cord injuries. All animals were assessed prior to injury for normal walking (score of 21 on BBB scale).

Retrovirus production and injection

A gammaretrovirus based on the murine leukemia virus (MLV) was used to transfect dividing cells. Retroviral encoding the green fluorescence protein (RV-GFP, Addgene # 16664) was produced by calcium chloride transient transfection into HEK293 cells, followed by supernatant viral purification by ultracentrifugation (Tashiro et al., 2006). Determination of viral titer was performed by serial dilution and visualization of colonies expressing GFP. The viral titer

obtained ranged from 0.5 to $1x10^9$ infections units per ml. The virus was aliquoted and stored in -80 °C until used.

For intraspinal injections, rats were anesthetized as above on day 1, 2, 7, 14, 21, or 28 post-injury and the laminectomy site was re-exposed (see **Table 2** for group details). A volume of 1μl of GFP-retrovirus solution was carefully drawn up into a sterile Hamilton syringe, which was gently inserted into the center of the lesion site. The solution was slowly injected into the spinal cord and the syringe maintained in place for an additional two minutes to prevent back-flux from the injection site. The surgery site was closed as above and animals returned to their home cages. Sham animals (n=4) that had received a laminectomy but no injury were similarly injected with the 1μl of GFP-retrovirus solution and sacrificed three weeks later.

Generation of PDGFαR-CreER:mT/mG transgenic mice

Since NG2 is expressed by pericytes and some macrophages after SCI, PDGFαR reporter mice were used for this study. *PDGFαR-CreER* transgenic mice have previously been described (for detailed information, see Supplementary information in Rivers et al., 2008). Heterozygous *PDGFαR-CreER* mice that were backcrossed with C57BL/6J mice for four generations were bred with mT/mG mice (Jackson Laboratories, strain B6.129(Cg)-Gt(ROSA)26Sor$^{tm4(ACTB-tdTomato,-EGFP)Luo}$/J) in which all cells ubiquitously express membrane-targeted tandem dimer Tomato (mT) prior to Cre-mediated recombination (Muzumdar et al., 2007) (**Fig 4A**). All mice used for experiments were Pdgf*αR*+ and heterozygous for mT/mG. After recombination, cells transcribing the PDGFαR promoter express membrane-targeted enhanced GFP (mG). Recombination was induced by oral administration of tamoxifen (300mg/kg) for four

consecutive days starting at 1, 14, 21, 28, or 42dpi and animals were sacrificed three weeks later (see **Table 2** for group details).

Generation of PDGFαR-ROSA transgenic mice

Heterozygous *PDGFαR-CreER* transgenic mice were also similarly crossed with *ROSA26-EYFP* mice (Jackson Laboratories, strain B6.129X1-*Gt(ROSA)26Sor*$^{tm1(EYFP)Cos}$/J) to generate *PDGFαR-ROSA* mice that express cytoplasmic GFP under the control of the PDGFαR promoter after recombination. Recombination was induced by oral administration of tamoxifen (200mg/kg) for four consecutive days starting at 28 or 52dpi, and animals were sacrificed at 52 and 80dpi (~7 and 12wpi), respectively (see **Table 2** for group details).

Tissue processing: Immunohistochemistry

For tissue collection, rats were deeply anesthetized with ketamine and xylazine (1.5X surgery dose above), and then perfused transcardially with PBS followed by 250ml of 4% paraformaldehyde in PBS. Spinal cords were removed, post-fixed for 2h at 4°C, and placed in 0.2M PB overnight. Tissue was cryoprotected in 30% sucrose at 4°C for 48h. For tissue embedding, spinal cords were frozen on dry ice and cut into 4mm blocks centered on the injection site. After submersion in OCT compound (Electron Microscopy Sciences), blocks were frozen, and cross sections were cut at 10μm on a cryostat and mounted onto slides. Tissue was stored at -20°C until used.

Immunohistochemistry

Sections were then rinsed in 0.1M PBS and blocked for nonspecific antigen binding using 4% BSA/0.1% Triton-100/PBS (BP^{+}) for 1h. Next, sections were incubated in primary antibody overnight at 4°C. Sections were rinsed and treated with horse biotinylated antiserum (horse anti-mouse IgG 1:800 in BP^{+}; Vector Laboratories) for 1h at room temperature. After rinsing, endogenous peroxidase activity was quenched using a 4:1 solution of methanol/30% hydrogen peroxide for 15 min in the dark. Sections were then treated with Elite avidin–biotin enzyme complex (ABC; Vector Laboratories) for 1h. Visualization of labeling was achieved using DAB or SG substrates (Vector Laboratories). Sections were rinsed, dehydrated, and coverslipped with Permount (Fisher Scientific). Sections were labeled with NG2 and Ki-67 to stain for oligodendrocyte progenitor cells and proliferating cells, respectively. For a complete list of antibodies used, see **Table 1.**

Immunofluorescence

Sections were rinsed in 0.1M PBS and blocked for nonspecific antigen binding using BP^{+} or 4% BSA/0.3% Triton-100/PBS (BP^{3+}) for 1h. Next, sections were incubated in primary antibody overnight at 4°C. Sections were rinsed and incubated with an AlexaFluor secondary antibody (1:500; Invitrogen) for 1h. For double- and triple-label immunofluorescence, sections were blocked and treated with primary and secondary antibodies, as above. After rinses, slides were coverslipped with Immu-Mount (Thermo Scientific). In cases where the primary antibody was raised in the same species as the tissue being labeled (mouse anti-CC1), the primary and secondary antibodies were first complexed together in 4%BSA/PBS/0.1andTx-100/0.3%NGS at

37°C for one hour, followed by the addition of normal mouse serum (1:500 dilution) for another hour, and then left on ice for 2 more hours.

Microscopy and quantitative analysis:

Immunofluorescent labeling was analyzed by confocal microscopy (Olympus FV1000 laser scanning confocal microscope) and Fluoview software. For quantification of fluorescent GFP+/CC1+ cells, nine non-overlapping images per spinal cord section (eight around the perimeter and one focused on the central canal) were collected at the epicenter, 0.15mm, and 0.45mm rostral and caudal to the injury site. The total number of GFP+/CC1+ cells from all nine images per section were summed and expressed as a fraction over the total area (μm^3) of spinal cord represented in the same images. A cell was counted if the CC1 label co-localized with DAPI and was completely surrounded by GFP labeling. A 2-way non-repeated measures ANOVA was used to analyze CC1/GFP+ cell counts with a Bonferroni post-hoc test, and significance was reported when $p<0.05$.

A Zeiss Axioskop 2 Plus microscope with a Sony 970 three-chip color camera was used to analyze non-fluorescent sections. Cells double-labeled for NG2 and Ki-67 were manually counted at high power (40X) throughout entire spinal cord cross sections. Cell counting was conducted in a conservative manner, and all cell counts are expressed as cells per mm^2. Criteria for a proliferating NG2 cell to be counted included a clearly defined border immunoreactive for NG2 surrounding an entire nucleus immunoreactive for Ki-67. These criteria had to be met in the same plane of focus. Care was taken to avoid counting NG2+ pericytes or macrophages, which are both easily distinguished by cellular morphology. A 1-way ANOVA was used to analyze

NG2/Ki-67+ cells counts where significance was reported when $p<0.05$.

Quantitative real-time PCR

cDNA was prepared from RNA isolated from mouse SCI tissue centered around the injury site as previously described using the Trizol method (Kigerl et al., 2007). Samples were collected at 1dpi, 3dpi, 1wpi, 2wpi, and 4wpi as well as from naïve tissue (n=4, 5, 5, 4, 5, 5, respectively). Levels of PCR product were measured using SYBR Green fluorescence. The primer sequences used were as follows: 18S(F) TTCGGAACTGAGGCCATGAT, (R) TTTCGCTCTGGTCCGTCTTG; Id2(F) GCTCTACAACATGAACGACTGCTACT, (R) TGCAGGTCCAAGATGTAATCGA; ID4(F) GAGACTCACCCTGCTTTGCT, (R) AGAATGCTGTCACCCTGCTT; Hes5(F) GCTGAGTGCTTTCCTATGAGGAA, (R) GCCCTGGGCACATTTGC; BMP2(F) CGTGCGCAGCTTCCATCACG, (R) GAAGAAGCGCCGGGCCGTTT; BMP4 (F) GCATCCGAGCTGAGAGACCCCA, (R) ATCCCATCAGGGACGGAGACCA. Data were analyzed using the Ct method (Livak & Schmittgen, 2001) and a one-way ANOVA with a Tukey post-hoc test. Significance was reported when $p<0.05$.

RESULTS

NG2 cells proliferate for 4 weeks after SCI, are maintained for at least 3 subsequent weeks and are located throughout the injured rat spinal cord

While several studies have shown that acutely dividing NG2 cells give rise to new OLs early after SCI, the long-term response and distribution of new NG2 cells is not known. To follow the fate of dividing NG2 cells after rat SCI, a one-time injection of a GFP-expressing retrovirus into the lesion was performed at different times post-injury and the rats allowed to survive an

additional 1 – 4 weeks (**Table 2**). This resulted in GFP expression by cells dividing at the time of virus injection, which allowed the fate of those cells to be followed over time.

To confirm that proliferating cells labeled by the GFP retrovirus could still be visualized 3-4 weeks later, virus was injected into the lesion at 1d or 2dpi and spinal cords examined at 28dpi. In this tissue, robust GFP labeling was present in cells throughout ~1cm of tissue centered on the injury epicenter (**Fig 1A**). GFP cells were present within the lesion cavity and in spared white and gray matter surrounding the injury site. To assure that the large number of GFP+ cells was not an artifact of the virus injection itself, GFP-retrovirus was injected into naïve rat spinal cords (n=4) and the tissue examined 3 weeks later. In contrast to the SCI tissue where GFP+ cells were present throughout ~1cm of tissue (**Fig 1A)**, GFP expression in naïve tissue was minimal and confined to ± 0.5mm around the injection site **(Fig 1B),** indicating that the injection stimulated only minor local proliferation.

The next step was to determine if proliferating NG2 cells would be labeled 1-4 weeks after virus injection. Thus, virus was injected at 1 or 2dpi (a time of robust NG2 cell proliferation) and spinal cords examined at 1wpi and 4wpi for GFP+ NG2 cells. At 1wpi, GFP+ NG2 cells were detected in all spinal cords examined, indicating that GFP-labeled NG2 cells dividing at 24 or 48h post-injury were maintained for 5-6 more days (**Fig 1C**).

A large number of GFP+ NG2 cells labeled at 1dpi persisted for 4wpi and were mainly located along lesion borders and in spared gray and white matter up to 4mm distal to the injury epicenter

(**Fig 1D E)**. Thus, a portion of NG2 cells proliferating at 1dpi at the lesion site are maintained for at least 4 weeks post-injury and distribute around and distal to the lesion.

To determine the fate of NG2 cells dividing at different times post-injury, GFP-retrovirus was injected into the spinal cord lesion of rats at 1, 2, 3, or 4wpi. Animals from each cohort survived an additional 3 weeks (i.e., 4-7wpi) and spinal cords were examined for the presence and distribution of GFP+ NG2 cells (**Table 2**). At every time examined, GFP+ NG2 cells were present throughout a 1cm segment of spinal cord centered on the injury site (**Fig 1F,G**). Thus, new NG2 cells are continuously produced between 1d and 4wpi and these new cells are present throughout the rostal-caudal extent of the injured spinal cord for at least 7wpi.

Although all spinal cords examined contained GFP+ NG2 cells, different distribution and numbers were observed based on time of virus injection. Most NG2 cells labeled at 1wpi accumulated 3 weeks later in a dense band along the lesion border/glial scar area, with fewer present in the spared white and gray matter around and distal to the lesion. A subset of GFP+ NG2s cells was also present within the lesion cavity. In tissue from later injections (e.g., virus at 4wpi, perfused at 7wpi), the overall number of GFP+ cells was lower than the 1week injection group and the dense accumulation of new NG2 cells along the lesion border did not occur. Rather, at 7wpi, GFP+ NG2 cells were primarily located near the border of lesions and distal spared white matter (**Fig 1C, G**). In summary, NG2 cells divide for at least 4wpi, the progeny of which survive and distribute throughout the injured and spared tissue surrounding the lesion after SCI. In addition, cells dividing more acutely appear to contribute to the formation of the glial scar.

To verify using a different technique that NG2 cells divide for 4wpi, tissue sections from each cohort were double-labeled for NG2 and Ki-67 and used to quantify NG2 cell proliferation at 1w, 2w, 3w, 4w, 6w and 10wpi. The number of NG2/Ki-67+ cells/mm^2 was significantly increased at the epicenter and ~1mm rostral and caudal to epicenter for 4wpi (**Fig 2A-C**). The number of double-labeled cells declined thereafter but still remained 3- to 9-fold above naïve levels at 10 weeks post-injury. Thus, these data verify that NG2 cells were dividing at each time of virus injection.

New OLs arise from cells dividing from 1d – 4 weeks post-injury in rats

While it is established that new OLs are generated 1-2 wpi, it is not known if more chronic lesion environments support OL differentiation. To compare oligodendrocyte genesis over time after SCI, tissue sections from rats injected with virus at 1dpi – 4wpi were examined for GFP+ OLs 3-4 weeks later. At every time point examined (4 to 7wpi), new OLs (GFP/CC1+ cells) were present in spared tissue surrounding the lesion (**Fig 3B-D**), indicating that cells dividing between 1d – 28dpi continuously differentiate into new OLs that remain for at least 7wpi

The distribution of new OLs was similar to that of GFP/NG2+ cells. That is, at 4wpi GFP/CC1+ cells were present along the lesion border as well as concentrated in the spared tissue around the lesion, which matches where GFP+ NG2 cells were located. At 7wpi, GFP+ OLs were more diffusely distributed; the majority of GFP/CC1+ cells were in distal spared tissue close to the meningeal border of the white matter. These results reveal that oligodendrogenesis occurs as late

at 4-7 weeks post-injury and that the pattern of NG2 cell proliferation predicts that of new OL generation.

Oligodendrogenesis continues for at least 80 days after SCI in mice

Since the SCI lesion pathology differs between rats and mice, two different reporter mouse lines were used to examine OL genesis after SCI in mice. Multiple cell types can express NG2, including pericytes and macrophages; therefore, reporter mice expressing GFP under the PDGF*α*R promoter were used, as this receptor is expressed specifically by OPCs. *PDGFαR-CreER:mT/mG* mice express membrane-bound GFP (mG) (Muzumdar et al., 2007) in PDGF*α*R+ cells after tamoxifen treatment, which allows fine cellular processes and newly formed myelin to be visualized (Kang et al., 2010; Powers et al., 2013) (**Fig 4A)**. The second line, *PDGFαR-CreER-ROSA* mice, express cytoplasmic GFP in PDGF*α*R+ cells upon Cre-recombination by tamoxifen. In both lines, GFP expression was induced in PDGF*α*R+ progenitors at different times post-injury and the fate of those cells examined 3 weeks later (**Table 2**).

To confirm efficient labeling of NG2 cells in *PDGFαR-CreER:mT/mG* mice, cross-sections of naïve spinal cords were immunolabeled for NG2. In these sections ~90% of GFP+ cells expressed NG2 and were present throughout white matter (**Fig 4B**) and gray matter (**Fig 4C**). To examine progenitor cell distribution and fate at different times after SCI, cohorts of *PDGFαR-CreER:mT/mG* mice were given a 4d regimen of tamoxifen starting at 1d, 2w, 3w, 4w, or 6w after SCI and sacrificed 3 weeks later (**Table 2**). A robust increase in the number of GFP+/NG2+ cells was present at every time examined (4w, 5w, 6w, 7w, and 9wpi) throughout the gray and white matter compared to naïve spinal cords. (**Fig. 4D-F**). A low power comparison between

naïve and 7wpi tissue illustrates the more robust GFP and NG2 expression in the injured tissue is maintained almost 2 months post-injury (**Fig 4G-H**). This demonstrates that expanded NG2 cell population is maintained long-term, as noted previously (McTigue et al., 2001; Rabchevsky et al 2007).

Generation of new OLs acutely after SCI has been detected in mice (Lytle & Wrathall, 2007). To determine if oligodendrogenesis continues chronically, sections from *PDGFαR-CreER:mT/mG* mice were examined for GFP+ OLs following tamoxifen administration as described above (**Table 2**). New OLs were generated during every time interval examined, including 1- 4w, 2 - 5w, 3 - 6w, 4 - 7w, and 6 - 9wpi. Numerous GFP+ OLs cells were present in spared white matter and gray matter in spinal cords in which GFP was turned on during every interval **(Fig 5A-D**). This reveals that progenitor cells differentiated into new OLs as late at between 6-9wpi. In longitudinal sections, GFP+ oligodendrocyte processes ran parallel to axons in spared white matter, resembling myelin profiles (**Fig 5D**).

To confirm the observation of chronic oligodendrogenesis in another mouse line and to examine a later time point after SCI, *PDGFαR-CreER-ROSA* mice were given tamoxifen 4w or 8wpi and sacrificed 4 weeks later (**Table 2**). In both groups, GFP+/CC1+ cells were prevalent throughout spared white and gray matter (**Fig 5E,F**), confirming that chronic oligodendrogenesis continues after mouse SCI and that OL progenitors as late as 8wpi differentiate into new OLs that survive for an additional month.

To quantify new OLs generated during the first, second and fourth weeks post-injury, tissue collected at 4, 5, and 7wpi from *PDGFαR-CreER-ROSA* mice was cut in cross-section and used to count new OLs at the epicenter and 0.15 and 0.45mm distal to the injury site. In uninjured spinal cords, only 1-2 GFP/CC1+ cells per section could be identified in naïve spinal cord tissue, which is consistent with a low rate of adult oligodendrogenesis in previous reports (Psachoulia et al., 2009). The number of new OLs were formed between 2-5wpi, with the fewest OLs at the epicenter (**Fig 6A**). The number of new OLs generated between 2-5wpi was significantly increased compared to naïve tissue, and to earlier and later tissue at rostral/caudal distances. When collapsed over distance, the number of new OLs formed between 2-5wpi was 120-fold greater than in uninjured spinal cords (**Fig 6B**). While the number of new OLs generated over 0-4wpi and 4-7wpi was lower than during 2-5, there still was a >40-fold increase during these time frames compared to uninjured spinal cords (**Fig 6B**).

New OL lineage cells ensheathe axons and demonstrate signs of functional remyelination as late as 7-9wpi

Rats injected with a GFP-retrovirus at 1d or 4wpi were immunolabeled for GFP, neurofilament (NF) and/or MBP and sacrificed at 4 or 7wpi, respectively. At 4wpi, GFP+ processes were commonly seen wrapping NF+ axons, some of which penetrated through the edges of the lesion cavity (**Fig 7A**). Z-stack analysis confirmed the co-localization of GFP, NF, and MBP on axons around the lesion border, indicating that newly formed OLs actively remyelinated axons (**Fig 7B-C**).

Similar observations were made in animals sacrificed at 7wpi. GFP+ processes co-localized with NF and MBP, indicating that OLs born from NG2 cells proliferating at 4 weeks post-injury were also able to myelinate axons (**Fig 7D**). Evidence of chronic remyelination in rats was bolstered by triple-labeling for GFP, NF, and the paranodal protein Caspr. Around the lesion border at 7wpi, GFP+ processes that wrapped NF+ axons were abutted adjacent to Caspr+ paranodal junctions, which are indicative of functional Nodes of Ranvier (**Fig 7E**). The number of GFP/NF/MBP+ and GFP/NF/Caspr+ axons was likely underestimated in the 6- and 7wpi animals as the uptake and spread of the GFP-retrovirus seemed to be diminished due to the lesion/scar tissue present at the time of injection.

PDGFαR-CreER:mT/mG mice revealed similar findings. In these mice, GFP+ processes of OL lineage cells co-localized with NF+ axons at all time points examined**,** specifically between 0-4 (**Fig 8A**), 3-6 (**B**), 4-7 (**C, D**), and 6-9wpi (**E, F**). These examples of GFP/NF+ processes were most often found along the meningeal borders of distal spared white matter of the spinal cord in mice. Tissue from 9wpi was also triple-labeled for GFP, NF, and Caspr+ (**Fig 8F**). Similar to rat tissue, Caspr+ paranodal junctions were present along NF+ axons, adjacent to GFP+ processes enwrapping the axon. The spacing between Caspr+ junctions was abnormally short, a hallmark of remyelination. Taken together, these observations in mice and rats indicate that new OLs are formed as late as 8 weeks after SCI and are capable of functional remyelination in the chronically injured spinal cord.

CNTF, FGF-2, and pSTAT3 expression are increased chronically in astrocytes after SCI in mice and rats

Previous work from our lab showed that CNTF and FGF-2 are increased for at least 28dpi along the gliogenic lesion border after SCI (Tripathi & McTigue, 2008). To extend these findings to more chronic time points, mouse tissue from 12wpi was first immunolabeled for CNTF and compared to naïve spinal cords. Minimal CNTF immunoreactivity was present in naïve mouse tissue in motor neurons and some white matter glial cells (**Fig 9A**). At 12wpi in mouse, CNTF labeling was much more robust, both in spared white matter (**Fig 9B**) and especially in the glial scar (**Fig 9B'**). The majority of CTNF was expressed by GFAP+ astrocytes (**Fig 9B' insert**), but not in OLs or NG2 cells (not shown).

Labeling of FGF-2 demonstrated a similar increase over time. In control rat tissue, there were a number of FGF-2+ cells primarily in the gray matter (**Fig 9C**). After injury, FGF-2 labeling increased and was present throughout the spared tissue around the lesion for at least 6wpi in rat (**Fig 9D**). FGF-2 did not colocalize with NG2 or CC1 at 5wpi (not shown), and was almost exclusively present in GFAP+ astrocytes (**Fig 9D' insert**).

Next, to get an indication of whether the CNTF pathway was active at 12wpi, pSTAT3 expression, which is downstream of CNTF signaling, was also analyzed. Naive mouse tissue contained virtually no pSTAT3+ cells (**Fig 9E**). In contrast, at 12wpi in mouse, there was an abundance of pSTAT3 labeling, which was localized primarily in GFAP+ astrocytes (**Fig 9F**). pSTAT3+ cells were particularly concentrated around the lesion border, but did not colocalize with NG2 or CC1 at 5wpi (not shown).

The expression of several NG2 cell fate-associated genes is chronically altered after SCI

cDNA gene expression of ID2, ID4, Hes5, BMP4, and BMP2 was analyzed by real time qPCR in epicenter SCI mouse tissue from 1d - 4wpi. ID2, ID4, and Hes5 are negative regulators of NG2 cell differentiation (Kondo & Raff, 2000; Samanta & Kessler, 2004; Li & Richardson, 2009). Expression of ID2 was significantly increased at 4wpi compared to naïve, 1dpi, 3dpi, and 7dpi (**Fig 10A**), while that of ID4 was significantly increased at both 2wpi and 4wpi compared to naïve, 1dpi, 3dpi, and 1wpi time points (**Fig 10B**). Conversely, expression of Hes5 was significantly decreased at 1dpi, 3dpi, 1wpi, and 4wpi compared to naïve levels (**Fig 10C**). BMP4, which regulates the expression of ID2 and ID4 (Samanta & Kessler, 2004), was significantly increased at 2wpi compared to 1dpi and at 4wpi compared to naïve, 1dpi, and 3dpi (**Fig 10D**). Expression of BMP2 was only significantly increased at 1dpi compared to all other time points examined (**Fig 10E**).

DISCUSSION

Recently, many therapeutic strategies following SCI have focused on promoting remyelination and protecting OL lineage cells (Mekhail et al., 2012). This is understandable considering the importance of myelin for proper axonal signal conduction as well as that of newly generated OLs to provide such remyelination. Independent of myelination, OLs are critical for maintaining axonal integrity and survival, perhaps even providing metabolic support to axons (Griffiths et al., 1998; Nave, 2010a; Nave 2010b; Lee et al., 2012). This emphasis on NG2 cell survival and their subsequent capacity for remyelination following SCI has been bolstered overtime by several NG2 cell-transplantation studies that have reported varying degrees of increased remyelination

and/or functional recovery (Keirstead et al., 2005; Karimi-Abdolrezaee et al., 2006; Cao et al., 2010; Plemel et al., 2011; Sun et al., 2013).

It is difficult, however, to anticipate the eventual outcomes of such interventions when little is actually known about the natural long-term fate of NG2 cells following SCI and how these cells behave in the chronic injury milieu. While it is known that NG2 cells spontaneously proliferate for at least 4wpi and that a significant increase in newly formed OLs can be observed by 2wpi (McTigue et al., 2001; Zai and Wrathall, 2005; Horky et al., 2006; Lytle et al., 2006; Tripathi and McTigue, 2007; Rabchevsky et al., 2007), a more comprehensive and detailed analysis of NG2 cell fate after these acute times points has not been previously conducted. Therefore, using *Cre-Er* technology and GFP-expressing retroviruses, we sought to track the long-term fate of NG2 cell after SCI to determine when different groups of NG2 cells proliferated, differentiated, and began to remyelinate. Due to the differences in lesion pathology between mice and rats after SCI, we also assessed chronic NG2 cell fate in both of these species, including comparisons between two different transgenic mouse lines. In this study we demonstrate the following conclusions: 1) NG2 cells surrounding the lesions proliferated significantly until 4wpi; 2) oligodendrogenesis occurred continuously for at least 56-80dpi (8-11.5wpi); 3) chronically formed OL lineage cells demonstrated signs of active and maintained remyelination; 4) pro-OL survival factors CNTF, FGF-2, and pSTAT3 were chronically upregulated around the lesion, primarily in astrocytes; and finally 5) genes associated with NG2 cell fate determination (BMP4, ID2, ID4, Hes5) were significantly altered long-term after SCI.

Chronic NG2 cell proliferation and oligodendrogenesis after SCI

The current results in mouse and rat revealed the chronic behavior of NG2/PDGFαR cells out to 11.5wpi. In *PDGFαR-CreER:mT/mG* mice, NG2 cells were labeled with GFP and tracked for three week periods during 0-4wpi, 2-5wpi, 3-6wpi, 4-7wpi, and 6-9wpi. During each of these times GFP+ cells were identified that either remained NG2+/PDGFRa+ during the entire period or become CC1+ OLs (**Figs 4 & 5**). Quantification from mice revealed that oligodendrogenesis was most robust between 2-5wpi, but oligodendrogenesis still occurred between the periods of 0-4, 3-6, 4-7, and 6-9wpi as well. It is possible that many more NG2 cells differentiated into OLs in the first two weeks after SCI, but did not survive to the 4wpi time point. In fact, Horky et al. (2006) reported that most dividing progenitor cells die in the first 24hrs after SCI. We then extended this study in *PDGFαR-CreER-ROSA* mice where we followed GFP+ cells during the periods of 4-7.5 and 8-11.5wpi and observed many GFP+/NG2+ and GFP+/CC1+ cells side-by-side throughout spared gray and white matter (**Fig 5f-g**). GFP-retrovirus studies in rat once again confirmed these observations (out to 7wpi) with the additional knowledge that any GFP+/NG2+ or GFP+/CC1+ cells seen had been actively proliferating at the time of viral injection (**Fig 1 & 3**). Taken together these three animals models present convincing evidence that oligodendrogenesis is an ongoing and chronic phenomenon, continuing for much longer and to greater extents than previously known.

Evidence for late-term remyelination after SCI

In addition to observing chronic oligodendrogenesis out to 80dpi, we also found evidence of on-going remyelination. In *PDGFαR-CreER:mT/mG* mice clear examples could be found where GFP+ processes wrapped and engaged NF+ axons at all time points examined (0-4wpi, 2-5wpi,

3-6dpi, 4-7wpi, and 6-9wpi) (**Fig 7**). These observations were again confirmed and extended in GFP-retrovirus tissue in rat where triple-labeling demonstrated co-localization of GFP, NF and MBP at 4 and 7wpi, even along the lesion cavity borders (**Fig 6**). We also found GFP+ processes that wrapped NF+ axons that ended in Caspr+ paranodal junctions, indicative of functional synapses (**Fig 6e**).

Long-term changes in transcription and astrocyte-derived growth factors correlate with oligodendrogenesis

Previous work from our lab showed that expression of CNTF, FGF-2, and pSTAT3 was elevated for at least 4wpi around the lesion border after SCI (Tripathi & McTigue, 2008). CNTF is an astrocyte-derived factor that is known to promote NG2 cell proliferation, differentiation, migration, and myelin formation, especially after injury, as well as protect OLs against TNFα toxicity (Barres et al., 1993, 1996; Mayer et al., 1994; Marmur et al., 1998; Talbott et al., 2007; Salehi et al, 2013; Vernerey et al., 2013). CNTF also initiates the phosphorylation of STAT3 and enhances the effects of FGF-2 which are important for oligodendrogenesis (Dell'Albani et al., 1998; Baron et al., 2000; Yokogami et al., 2000). It has also been suggested that activation of the STAT3 pathway in astrocytes after brain injury in both humans and rodents may help to prevent impairment of oligodendrocyte maturation (Nobuta et al., 2012). Thus, we examined the expression of these factors in our chronically injured tissue. We found that that expression of CNTF was still increased until at least 11.5wpi in mice and that of FGF-2 and pSTAT3 until at least 6wpi in rat (**Fig 9**). These factors were found almost exclusively in astrocytes. The chronic presence of these pro-OL proteins may contribute to the late-term oligodendrogenesis seen after

SCI and indicate that the injury environment contains factors permissive to OL maturation and survival.

qPCR was also performed on genes associated with NG2 cell fate determination (**Fig 10**). ID2, ID4, and Hes5 are known inhibitors of oligodendrogenesis (Kondo & Raff, 2000; Samanta & Kessler, 2004; Li & Richardson, 2009). ID2 and ID4 do so by directly inhibiting the expression of Olig1 and Olig2 (Gokhan et al., 2005; Chen et al., 2009) while Hes5 inhibits Sox21 expression (Wen et al., 2009). While expression of ID2 and ID4 was only increased at 2 or 4wpi, expression of Hes5 remained chronically downregulated from 1dpi until at least 4wpi. Thus, increases in ID2 and ID4 expression at 4wpi may contribute to a reduction in the rate of oligodendrogenesis at more chronic time points, but consistently decreased expression of Hes5 may still be favorable for continual NG2 cell differentiation. Expression of BMP4, which regulates that of ID2 and ID4, increased in a similar time-dependent manner as these two factors (Samanta & Kessler, 2004). In contrast, expression of BMP2 was only significantly elevated at 1dpi. BMP2 and BMP4 are also considered to be inhibitors of oligodendrogenesis, and it has been shown that these factors can influence NG2 cells to take on an astrocytic fate, both in development and in the adult (See et al., 2004; Cheng et al., 2007; Porlan et al., 2013). Conversely, others have shown that injection of BMP4 into the injured spinal cord can reduce astrogliosis (Sellers et al., 2009). As the entire epicenter of the injured mouse cord was used for qPCR analysis, it is not possible to ascertain which cell types are expressing these transcription factors. However, it is interesting to note that holistic expression changes in ID2, ID4, Hes5, and BMP4 are only seen or are maintained at chronic time points after SCI. These long-term gene

changes contribute to the idea of a chronically dynamic environment after SCI with undergoes significant structural and cellular changes long after acute injury effects have subsided.

Therapeutic implications of chronic oligodendrogenesis after SCI

The work presented here demonstrates that the injured cord's capacity for oligodendrogenesis and subsequent remyelination, in both rats and mice, is greater in duration than previously known. In light of the dynamic changes involving oligodendrogenesis and remyelination that are still present at 11.5wpi (some of which may just be beginning), the appropriate time frame for therapeutic interventions directed at OL lineage cells should be reconsidered. This knowledge may both extend the window of opportunity for remyelination-promoting therapies as well as caution against intervening too soon due to the long-term dynamic cell changes that continue to occur. For example, insight into the chronic injury milieu is crucial for predicting how strategies such as stem cell transplantation will fare long-term or whether therapeutically-induced regenerated axons will become myelinated. Further, if protracted OL generation is crucial for lesion stabilization and chronic axon function, it will be important to understand the dynamics of this response so that pharmaceutical-based strategies do not interfere with this endogenous reparative response. Lastly, knowing that progenitor cells are responsive to environmental cues that promote oligodendrogenesis may provide new targets for treatments aimed at enhancing myelination, either of spared axons or axons induced to regenerate.

Acknowledgements: Images presented in this report were generated using the instruments and services at the Campus Microscopy and Imaging Facility, The Ohio State University. The authors declare no competing financial interests. We would like to thank Ping Wei and Andrea

Houchin for excellent technical assistance and Dr. Bill Richardson for his gift of the *PDGFαR-CreER* transgenic mice.

FIGURES

Primary antibody: specifity	Concentration	Host species	Vendor
Caspr: functional paranodal junctions	1/3000	Rabbit	AbCam
CC1: mature oligodendrocytes	1/100	Mouse	AbCam
CNTF: ciliary neurotrophic factor	1/100	Goat	R&D
FGF-2: fibroblast growth factor-2	1/500	Mouse	Upstate Charlottesville, VA
GFAP: astrocytes	1/10,000	Rabbit	Dako
GFP: green fluorescent protein	1/800	Chicken	Aves
Ki-67: proliferating cells	1/100	Mouse	Dako
MBP: mature myelin	1/500	Mouse	AbCam
	1/500	Chicken	Aves
NF: axons	1/1000	Chicken	Aves
	1/500	Mouse	DSHB
NG2: progenitor cells	1/500	Rabbit	USBiological
	1/200	Mouse	USBiological
pSTAT3: phosphorylated STAT3	1/200	Rabbit	Cell Signaling

TABLE 1: List of all primary antibodies used in this study.

Table 2: Animal Groups

Rat		
GFP-Virus	*Sac date*	*n*
1d or 2d	1w	6
1d	4w	8
7d	4w	4
14d	5w	4
21d	6w	4
28d	7w	5
PDGFRa-ROSA mice		
Tamox	*Sac date*	*n*
28-31d	7w	4
56-59d	11w	6
mTmG mice		
Tamox	*Sac date*	*n*
1-4d	4w	4
1-4d (TEM)	4w	3
14-17d	5w	5
21-24d	6w	2
28-31d	7w	5
42-45d	9w	3

TABLE 2: Animal number and time course information.

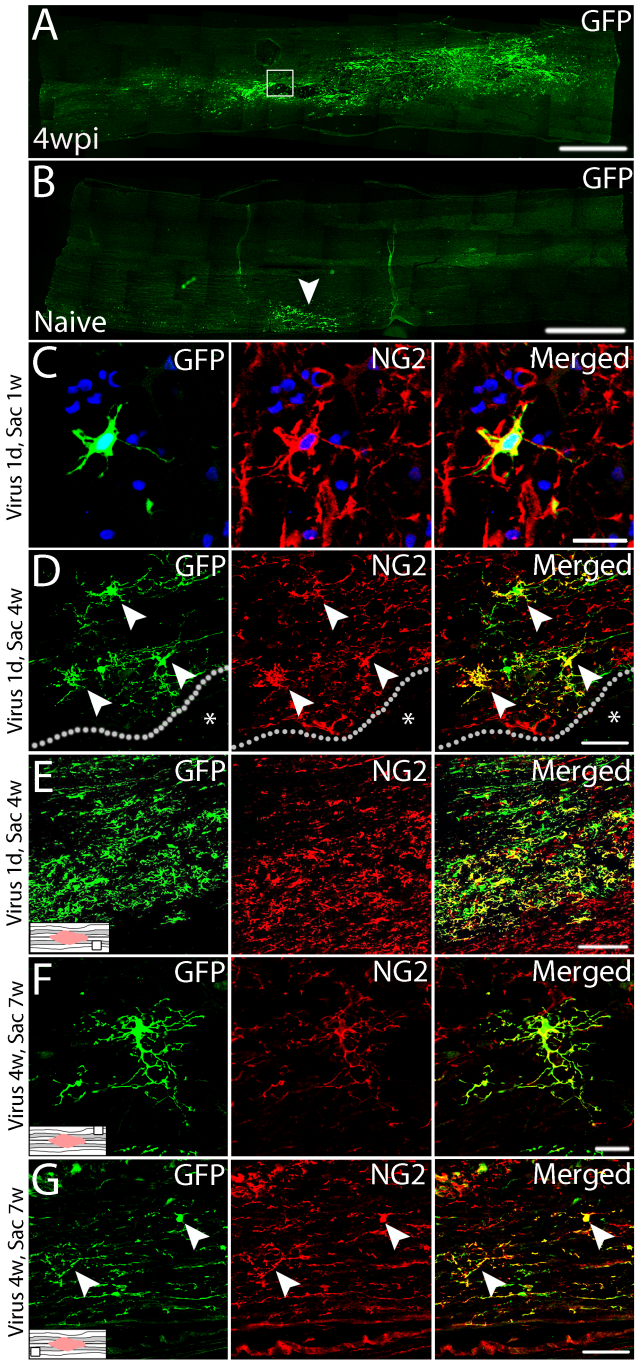

FIGURE 1: Intraspinal injection of GFP-retrovirus successfully labels proliferating NG2 cells after SCI in rat. **A**. Widespread GFP-expression in the spinal cord at 4wpi (virus at 1dpi). **B**. In naïve cord, intraspinal injection stimulates only a small amount of cellular proliferation (GFP+ cells) around the injection site which does not spread throughout the cord. Examples of

GFP+/NG2+ cells at 1wpi (**C**), 4wpi (**D, E**), and 7wpi (**F, G**) at various locations throughout the spinal cord. (**D**) is a close up of the white box in (**A**). Location within the spinal cord where images were taken is indicated by associated schematics. DAPI is labeled in blue. Scale bars = 20µm (**A**); 150µm (**B**); 50µm **(C)**; 1250µm (**D, E**); 50µm (**F, G**).

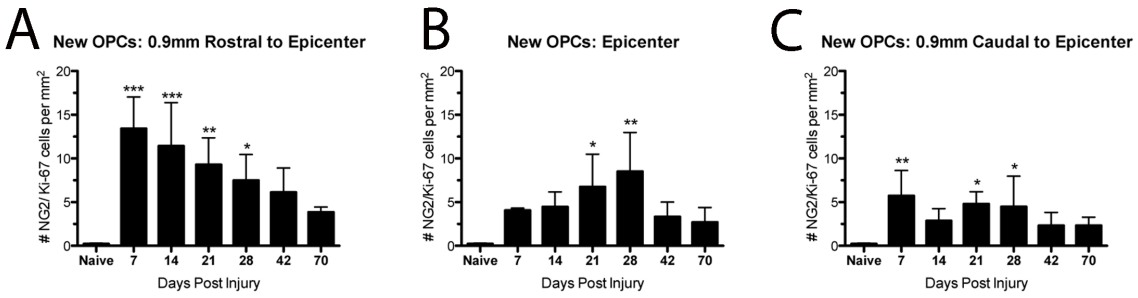

FIGURE 2: Number of Ki-67+/NG2+ cells in the rat spinal cord rostral to the epicenter (**A**), at the epicenter (**B**), and caudal to the epicenter (**C**) until 70dpi. Significance is in comparison to naïve counts.

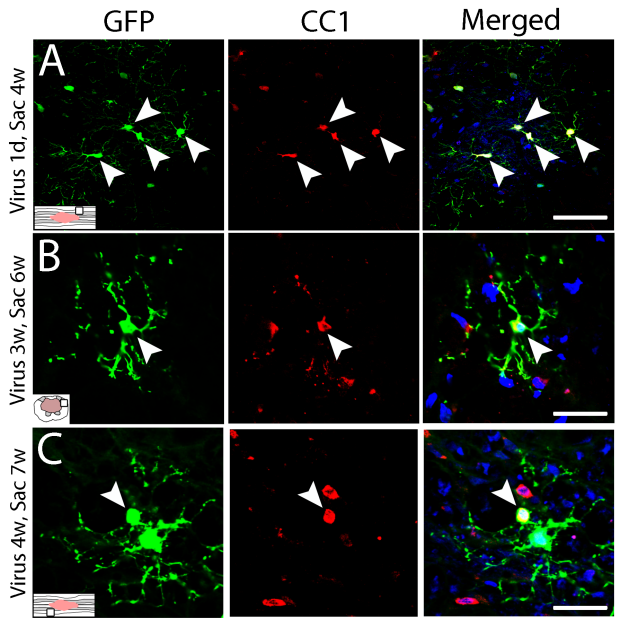

FIGURE 3: Chronic oligodendrogenesis from proliferating progenitors in the injured rat spinal cord. Examples of GFP+/CC1+ cells around the lesion area at 4wpi (**A**), 6wpi (**B**), and 7wpi (**C**). DAPI is labeled in blue. Scale bars = 50µm (**A**, **B**); 30µm (**C**).

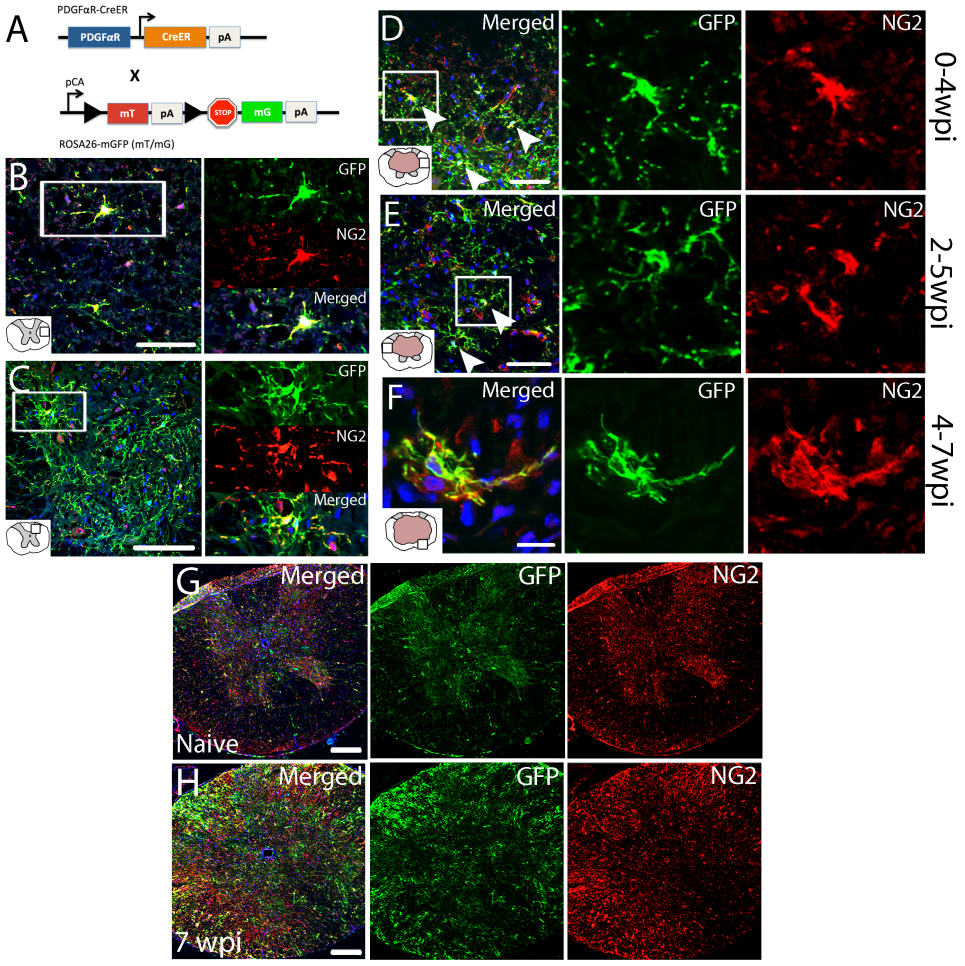

FIGURE 4: *PDGFαR-CreER:mT/mG* reporter mice successfully label NG2 cells that can be followed for at least 3 weeks after recombination. **A**. Schematic of breeding paradigm to generate *PDGFαR-CreER:mT/mG* mice. *PDGFαR-CreER* mice were crossed with *ROSA26-mGFP* (mT/mG) mice to generate mice that ubiquitously express membrane-targeted tandem dimer Tomato (mT). Upon recombination by oral administration of tamoxifen however, all cells expressing the PDGFαR promoter begin to express membrane-targeted GFP (mG). pCA = promotor with CMV enhancer; pA = polyadenylation sequences; arrows = direction of transcription. Examples of GFP+/NG2+ cells in naïve spinal cord white (**B**) and gray **(C**) matter. Examples of GFP+/NG2+ around the lesion area of injured spinal cord at 4wpi (**D**), 5wpi (**E**),

and 7wpi (**F**). Low-power visual comparison of naïve (**G**) and injured spinal cord (7wpi) (**H**) labeled with GFP and NG2. Even at 7wpi, GFP/NG2 expression is still considerably increased in the injured tissue. The injured tissue in (**H**) is 250µm rostral from the epicenter with no apparent signs of lesion. DAPI is labeled in blue. Scale bars = 50µm (**B, D, E**); 100µm (**C, G, H**); 10µm (**F**).

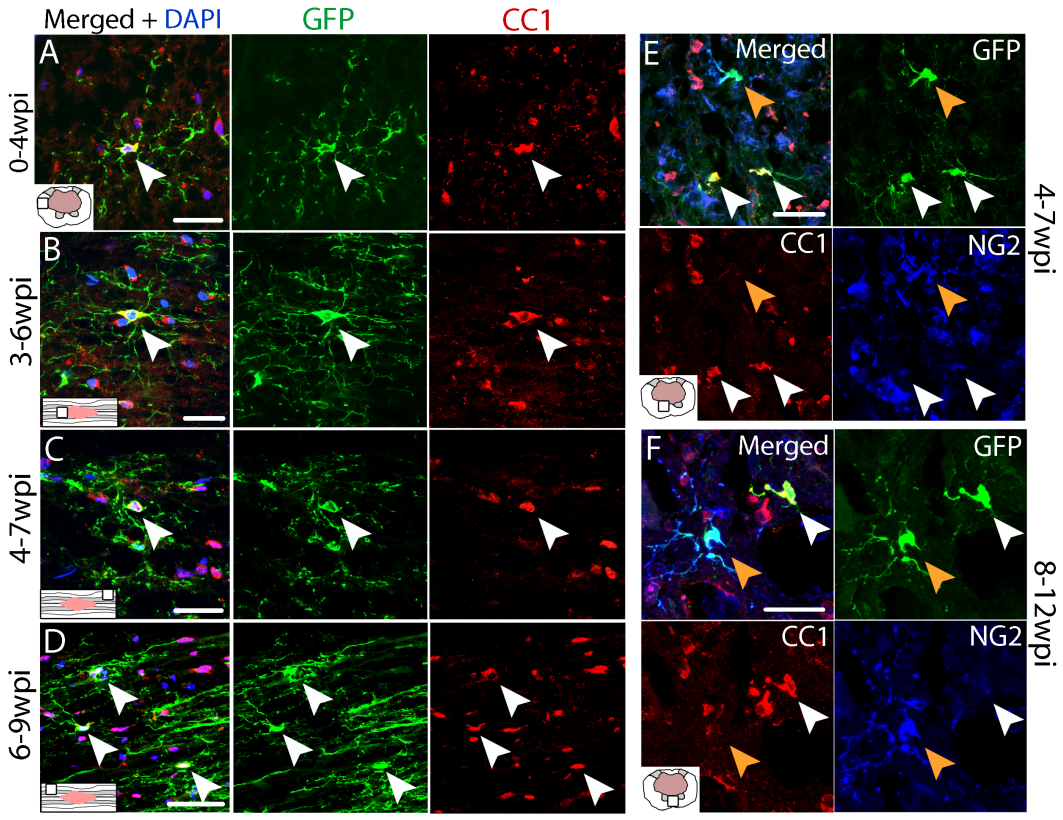

FIGURE 5: Chronic oligodendrogenesis occurs after SCI in mice until at least 12wpi. Examples of GFP+/CC1+ cells in *PDGFαR-CreER:mT/mG* mice at 4wpi (**A**), 6wpi (**B**), 7wpi (**C**), and 9wpi (**D**). Examples of GFP+/NG2+ and GFP+/CC1+ cells in *PDGFαR-ROSA* mice at 7.5wpi [52dpi] (**E**) and 11.5wpi [80dpi] (**F**). DAPI is labeled in blue. Scale bars = 30µm (**A, E, F**); 20µm (**B, C**); 50µm (**D**).

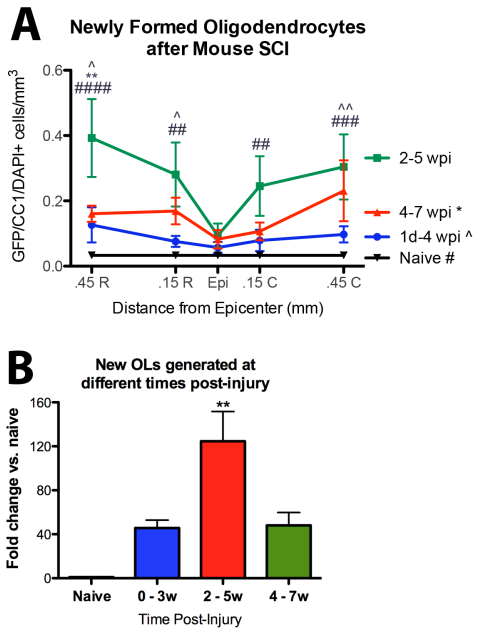

FIGURE 6: **A.** Quantification of newly formed OLs after SCI in *PDGFαR-CreER:mT/mG* mice between the periods of 0-4wpi, 2-5wpi, and 4-7wpi at the epicenter and rostral and caudal to the lesion. The number of newly formed OLs (GFP/CC1/DAPI+ cells) between 2-5wpi was significantly greater than in naïve tissue at 0.15mm and 0.45mm rostral and caudal to the epicenter, as well as compared to 0-4wpi (at 0.45mm rostral and caudal and 0.15mm rostral to the epicenter) and 4-7wpi (0.45mm rostral to the epicenter only). The number of triple-labeled cells was always lowest at the epicenter.

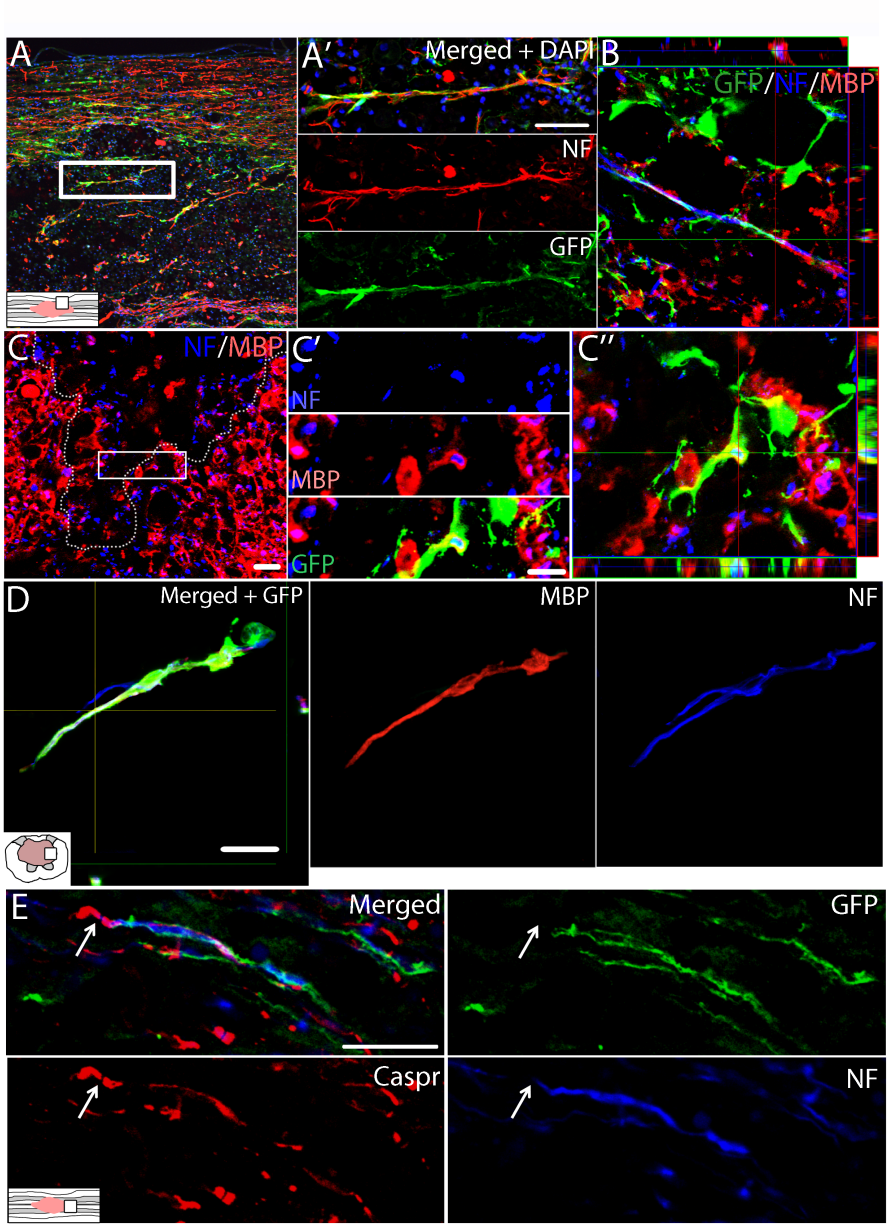

FIGURE 7: Proliferating OL lineage cells engage axons and express markers of functional remyelination after SCI in rat. **A.** Spinal cord tissue at 4wpi (virus injected at 1dpi) labeled with GFP and NF. (**A'**) A GFP+ processes ensheathes a NF+ axons extending into the lesion cavity. At 4wpi, GFP+ processes wrap NF+ axons and also colocalize with MBP around the lesion border (**B-C**). These images (**A-C**) represent NG2 cells that were proliferating at 1dpi and then

matured into OLs within 4 weeks that express mature myelin proteins and contribute to remyelination. **D**. Spinal cord tissue at 7wpi (virus injected at 4wpi) that also demonstrate remyelination by colocalization of GFP+ processes with NF+ axons and MBP within the lesion cavity. **E.** A GFP+ process from an OL lineage cell in 7wpi rat tissue that wraps a NF+ axon and ends in two adjacent Caspr+ paranodal junctions. Scale bars = 50µm (**A, C**); 20µm (**D, E**).

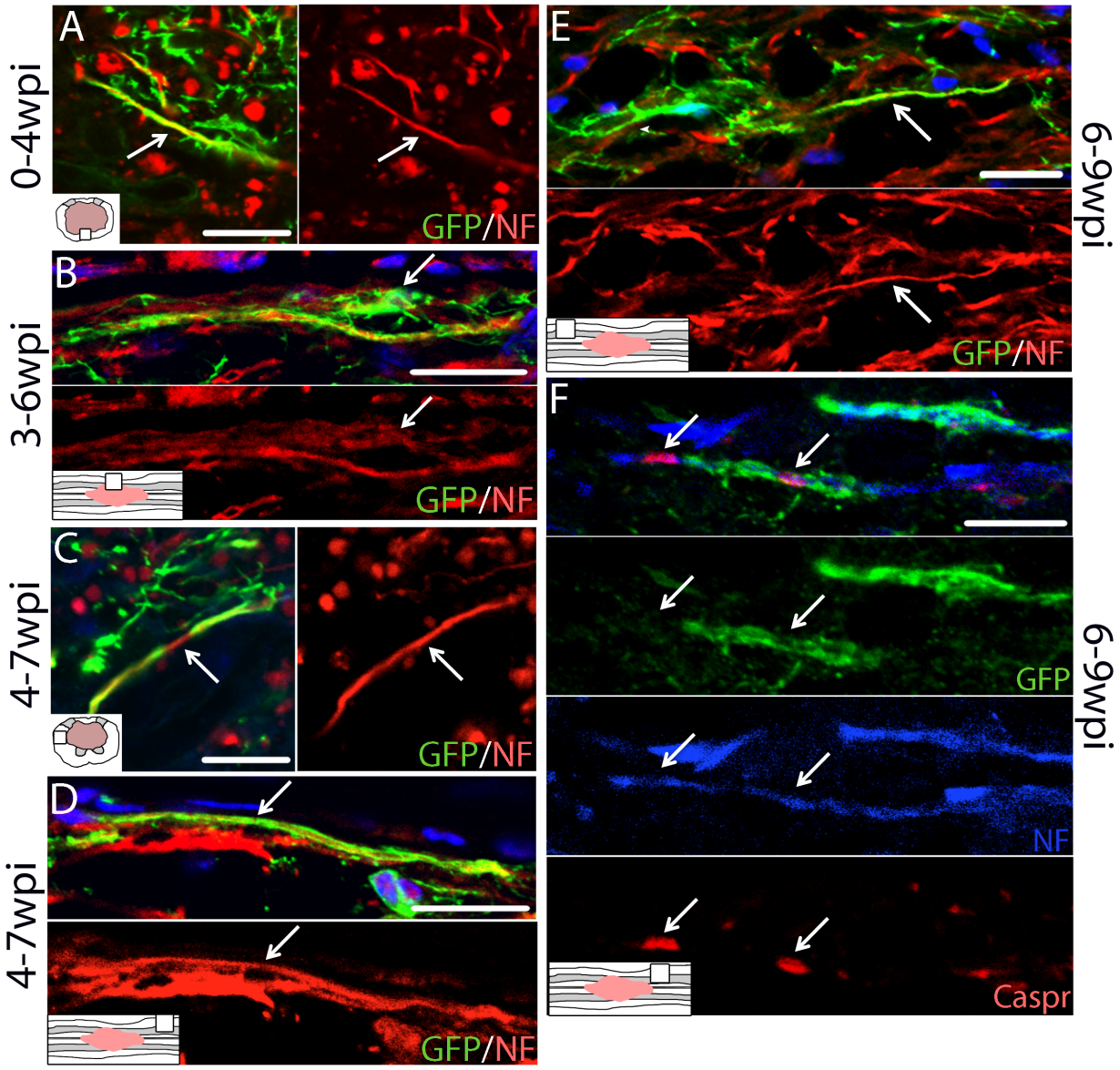

FIGURE 8: OL lineage cells continually wrap Caspr+ axons from 0-9wpi in mouse SCI tissue. GFP+ processes colocalize with NF+ axons during the time periods of 0-4wpi (**A**), 3-6wpi (**B**), 4-7wpi (**C, D**), and 6-9wpi (**E**). Examples in (**B**) and (**D**) clearly demonstrate the sheaths that GFP+ processes form around axons. The image in (**B**) also shows the adjacent OL lineage cell that gives rise to the GFP+ processes wrapping a NF+ axon. Examples of GFP/NF colocalization could be found in both spared white matter (**C, D, E**) as well as along lesion borders (**A, B**). **F**. GFP+ processes in 9wpi tissue wrap NF+ axons that express Caspr+ paranodal junctions. DAPI is labeled in blue except in (**F**). Scale bars = 10μm (**A, C, E, F**); 20μm (**D**); 30μm (**B, E**).

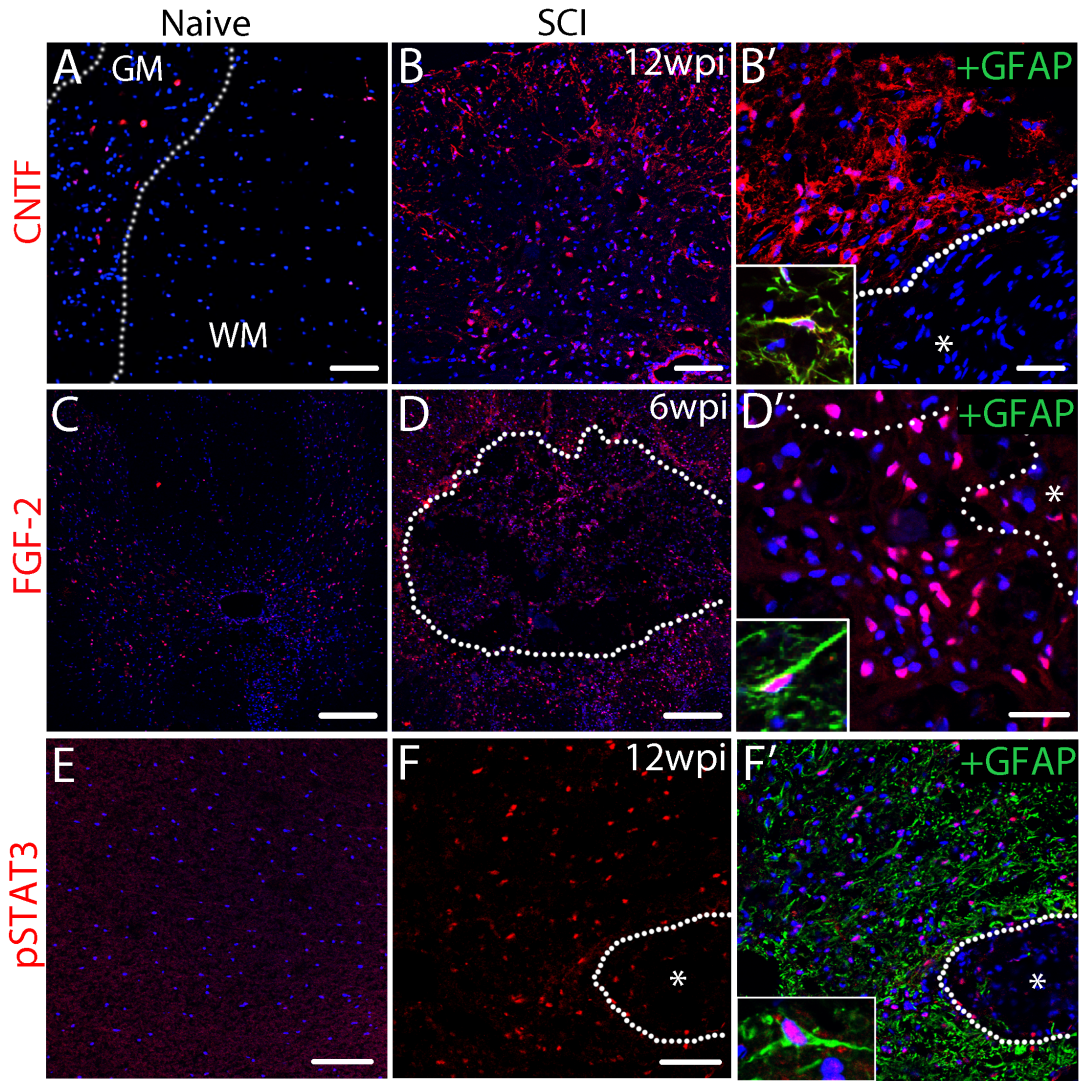

FIGURE 9: Chronic increases in CNTF, FGF-2, and pSTAT3 after SCI in mice and rats. **A**. Naïve *PDGFαR-ROSA* mice spinal cord tissue shows very little labeling of CNTF. **B**. At 11.5wpi, robust CNTF is still present in *PDGFαR-ROSA* mice. CNTF expression is primarily found on astrocytes, especially around the lesion border (**B'**). **C**. Expression of FGF-2 in naïve rat spinal cord is restricted to the gray matter. **D**. At 6wpi in rat, expression of FGF-2 is upregulated and spread more diffusely throughout spared gray and white matter as well as within the lesion cavity. Like CNTF, FGF-2 expression is primarily found on astrocytes, especially around the lesion border (**D'**). **E**. In naïve mouse spinal cord there is virtually no expression of pSTAT3. **F.** At

12wpi in mouse, pSTAT3 is still upregulated and found primarily within astrocytes (**F'**). DAPI is labeled in blue. Scale bars = 100μm (**A, B, E, F, F'**); 50μm **(B');** 200μm **(C, D, D').**

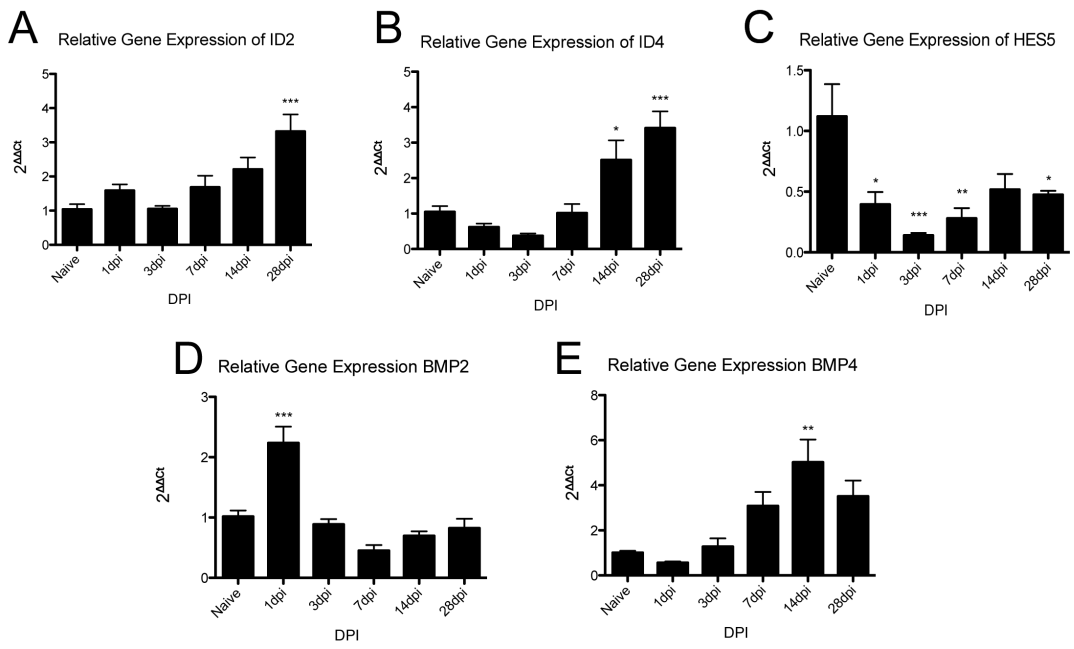

Figure 10: NG2 cell fate genes are chronically modulated after SCI. Relative gene expression of ID2 (**A)**, ID4 (**B**), Hes5 (**C**), BMP2 (**D**), and BMP4 (**E**). **A.** Expression of ID2 is significantly increased at 28dpi (*) compared to naïve levels. **B**. Expression of ID4 is significantly increased at both 14dpi (*) and 28dpi (***) compared to naïve levels. **C**. Expression of Hes5 is significantly decreased compared to naïve levels at 1dpi (*), 3dpi (***), 7dpi (**), and 28dpi (*). **D**. Expression of BMP2 is significantly increased compared to naïve levels at 1dpi (*). **E**. Expression of BMP4 is significantly increased at 14dpi (**) compared to naïve levels.

References:

Almad A, Sahinkaya FR, McTigue DM (2011) Oligodendrocyte fate after spinal cord injury. *Neurotherapeutics* 8(2):262-273.

Barnabé-Heider F, Göritz C, Sabelström H, Takebayashi H, Pfrieger F, Meletis K, Frisén J (2010) Origin of new glial cells in intact and injured adult spinal cord. *Cell Stem Cell* 7(4):470-482.

Baron W, Metz B, Bansal R, Hoekstra D, de Vries H (2000) PDGF and FGF-2 signaling in oligodendrocyte progenitor cells: regulation of proliferation and differentiation by multiple intracellular signaling pathways. *Mol Cell Neurosci* 15:314-329.

Barres BA, Schmid R, Sendnter M, Raff MC (1993) Multiple extracellular signals are required for long-term oligodendrocyte survival. *Development* 118:283-295.

Barres BA, Burne JF, Holtmann B, Thoenen H, Sendtner M, Raff MC (1996) Ciliary neurotrophic factor enhances the rate of oligodendrocyte generation. *Mol Cell Neurosci* 8:146-156.

Cao Q, He Q, Wang Y, Cheng X, Howard RM, Zhang Y, DeVries WH, Shields CB, Magnuson DS, Xu XM, Kim DH, Whittemore SR (2010) Transplantation of ciliary neurotrophic factor-expressing adult oligodendrocyte precursor cells promotes remyelination and functional recovery after spinal cord injury. *J Neurosci* 30(8):2989-3001.

Cheng X, Wang Y, He Q, Qiu M, Whittmore SR, Cao Q (2007) Bone morphogenetic protein signaling and olig1/2 interact to regulate the differentiation and maturation of adult oligodendrocyte precursor cells. *Stem Cell* 25(12):3204-3214.

Crowe MJ, Bresnahan JC, Shuman SL, Masters JN, Beattie MS (1997) Apoptosis and delayed degeneration after spinal cord injury in rats and monkeys. *Nat Med* 3(1):73-76.

Dawson MR, Polito A, Levine JM, Reynolds R (2003) NG2-expressing glial progenitor cells: an abundant and widespread population of cycling cells in the adult rat CNS. *Mol Cell Neurosci* 24(2):476-788.

Dell'Albani P, Kahn MA, Cole R, Condorelli DF, Giuffrida-Stella Am, de Vellis J (1998) Oligodendroglial survival factors, PDGF-AA and CNTF, activate similar JAK/STAT signaling pathways. *J Neurosci Res* 54:191-205.

Gledhill RF, Harrison BM, McDonald WI (1973) Demyelination and remyelination after acute spinal cord compression. *Exp Neurol* 38(3):472-487.

Griffiths I, Klugmann M, Anderson T, Yool D, Thomson C, Schwab MH, Schneider A, Zimmermann F, McCulloch M, Nadon N, Nave KA (1998) Axonal swellings and degeneration in mice lacking the major proteolipid of myelin. *Science* 280(5369):1610-1613.

Grossman SD, Rosenberg LJ, Wrathall JR (2001) Temporal-spatial pattern of acute neuronal and glial loss after spinal cord contusion. *Exp Neurol* 168(2):273-282.

Horky LL, Galimi F, Gage FH, Horner PJ (2006) Fate of endogenous stem/progenitor cells following spinal cord injury. *J Comp Neurol* 498:525-538.

Horner PJ, Thallmair M, Gage FH (2002) Defining the NG2-expressing cell of the adult CNS. *J Neurocytol* 31:469-480.

Hughes E, Kang SH, Fukaya M, Bergles DE (2013) Oligodendrocyte progenitors balance growth with self-repulsion to achieve homeostasis in the adult brain. *Nat Neurosci* 16(6):668-676.

Kang SH, Fukaya M, Yang JK, Rothstein JD, Bergles DE (2010) $NG2^+$ CNS glial progenitors remain committed to the oligodendrocyte lineage in postnatal life and following neurodegeneration. *Neuron* 68:668-681.

Karimi-Abdolrezaee S, Eftekharpour E, Wang J, Morshead CM, Fehlings MG (2006) Delayed transplantation of adult neural precursor cells promotes remyelination and functional neurological recovery after spinal cord injury. *J Neurosci* 26(13):3377-3389.

Keirstead HS, Blakemore WF (1997) Identification of post-mitotic oligodendrocytes incapable of remyelination within the demyelinated adult spinal cord. *J Neuropathol Exp Neurol* 56(11):1191-1201.

Keirstead HS, Nistor G, Bernal G, Totoiu M, Cloutier F, Sharp K, Steward O (2005) Human embryonic stem cell-derived oligodendrocyte progenitor cell transplants remyelinate and restore locomotion after spinal cord injury. *J Neurosci* 25(19):4694-4705.

Kigerl KA, Lai W, Rivest S, Hart RP, Satoskar AR, Popovich PG (2007) Toll-like receptor (TLR)-2 and TLR-4 regulate inflammation, gliosis, and myelin sparing after spinal cord injury. *J Neurochem* 102(1):37-50.

Kondo T, Raff M (2000) Basic helix-loop-helix proteins and the timing of oligodendrocyte differentiation. *Development* 127:2989-2998.

Rabchevsky AG, Sullivan PG, Scheff SW (2007) Temporal-spatial dynamics of oligodendrocyte and glial progenitor cell numbers throughout ventrolateral white matter following contusion spinal cord injury. *Glia* 55:831-843.

Richardson WD, Young KM, Tripathi RB, McKenzie I (2011) NG2-glia as multipotent neural stem cells – fact or fantasy? *Neuron* 70(4):661-673.

Rivers LE, Young KM, Rizzi M, Jamen F, Psachoulia K, Wade A, Kessaris N, Richardson WD (2008) PDGFRA/NG2 glia generate myelinating oligodendrocytes and piriform projection neurons in adult mice. *Nat Neurosci* 11:1392-1401.

Lee Y, Morrison BM, Li Y, Lengacher S, Farah MH, Hoffman PN, Liu Y, Tsingalia A, Jin L,

Zhang PW, Pellerin L, Magistretti PJ, Rothstein JD (2012) Oligodendroglia metabolically support axons and contribute to neurodegeneration. *Nature* 487(7408):443-448.

Livak KJ, Schmittgen TD (2001) Analysis of relative gene expression data using real-time quantitative PCR and the 2(-Delta Delta C(T)) Method. *Methods* 25:402-408.

Lytle JM, Vicini S, Wrathall JR (2006) Phenotypic changes in NG2+ cells after spinal cord injury. *J Neurotrauma* 23:1726-1738.

Lytle JM, Wrathall JR (2007) Glial cell loss, proliferation and replacement in the contused murine spinal cord. *Eur J Neurosci* 25(6):1711-1724.

Lytle JM, Chittajallu R, Wrathall JR, Gallo V (2009) NG2 cell response in the CNP-EGFP mouse after contusive spinal cord injury. *Glia* 57:270-285.

Marmur R, Kessler JA, Zhu G, Gokhan S, Mehler MF (1998) Differentiation of oligodendroglial progenitors derived from cortical multipotent cells requires extrinsic signals including activation of gp130/LIFbeta receptors. *J Neurosci* 18:9800-9811.

Mayer M, Bhakoo K, Noble M (1994) Ciliary neurotrophic factor and leukemia inhibitory factor promote the generation, maturation and survival of oligodendrocytes in vitro. *Development* 120:143-153.

McTigue DM, Wei P, Stokes BT (2001) Proliferation of NG2-positive cells and altered oligodendrocyte numbers in the contused rat spinal cord. *J Neurosci* 21:3392-3400.

McTigue DM, Tripathi R, Wei P (2006) NG2 colocalized with axons and is expressed by a mixed cell population in spinal cord lesion. *J Neuropathol Exp Neurol*, 65(4):406-420.

Mekhail M, Almazan G, Tabrizian M (2012) Oligodendrocyte-protection and remyelination post-spinal cord injuries: a review. *Prog Neurobiol* 96(3):322-339.

Muzumdar MD, Tasic B, Miyamichi K, Li L, Luo L (2007) A global double-fluroescent Cre

reporter mouse. *Genesis* 45:593-605.

Nave KA (2010a) Myelination and support of axonal integrity by glia. *Nature* 468(7321):244-252.

Nave KA (2010b) Myelination and the trophic support of long axons. *Nat Rev Neurosci* 11(4):275-283.

Nishiyama A, Lin XH, Giese N, Heldin CH, Stallcup WB (1996) Co-localization of NG2 proteoglycan and PDGF alpha-receptor on O2A progenitor cells in the developing rat brain. *J Neurosci Res* 43(3):299-314.

Nishiyama A, Komitova M, Suzuki R, Zhu X (2009) Polydendrocytes (NG2 cells): multifunctional cells with lineage plasticity. *Nat Rev Neurosci* 10:9-22.

Nobuta H, Ghiani CA, Paez PM, Spreuer V, Dong H, Korsak RA, Manukyan A, Li J, Vinters HV, Huang EJ, Rowitch DH, Sofroniew MV, Campagnoni AT, de Vellis J, Waschek JA (2012) STAT3-mediated astrogliosis protects myelin development in neonatal brain injury. *Ann Neurol* 72(5):750-765.

Plemel JR, Chojnacki A, Sparling JS, Liu J, Plunet W, Duncan GJ, Park SE, Weiss S, Tetzlaff W (2011) Platelet-derived growth factor-responsive neural precursors give rise to myelinating oligodendrocytes after transplantation into the spinal cords of contused rats and dysmyelinated mice. *Glia* 59(12):1891-1910.

Porlan E, Morante-Redolat JM, Marqués-Torrejón MA, Andreu-Agulló C, Carneiro C, Gómez-Ibarlucea E, Soto A, Vidal A, Ferrón SR, Farinas I (2013) Transcriptional repression of Bmp2 by p21Waf1/Cip1 links quiescence to neural stem cell maintenance. *Nat Neurosci* 16:1567-1575.

Powers BE, Sellers DL, Lovelett EA, Cheung W, Aalami SP, Zapertov N, Maris DO, Horner PJ

(2013) Remyelination reporter reveals prolonged refinement of spontaneously regenerated myelin. *Proc Natl Acad Sci* 110(10):4075-4080.

Psachoulia K, Jamen F, Young KM, Richardson WD (2009) Cell cycle dynamics of NG2 cells in the postnatal and ageing brain. *Neuron Glia Biology* 5:57-67.

Salehi Z, Hadiyan SP, Navidi R (2013) Ciliary neurotrophic factor role in myelin oligodendrocyte glycoprotein expression in Cuprizone-induced multiple sclerosis mice. *Cell Mol Neurobiol* 33:531-535.

Samanta J, Kessler JA (2004) Interactions between ID and OLIG proteins mediate the inhibitory effects of BMP4 on oligodendroglial differentiation. *Development* 131:4131-4142.

See J, Zhang X, Eraydin N, Mun SB, Mamontov P, Golden JA, Grinspan JB (2004) Oligodendrocyte maturation is inhibited by bone morphogenetic protein. *Mol Cell Neurosci* 26(4):481-492.

Sellers DL, Maris DO, Horner PJ (2009) Postinjury niches induce temporal shifts in progenitor fates to direct lesion repair after spinal cord injury. *J Neurosci* 29(20:6722-6733.

Sun Y, Xu CC, Li J, Guan XY, Gao L, Ma LX, Li RX, Peng YW, Zhu GP (2013) Transplantation of oligodendrocyte precursor cells improves locomotor deficits in rats with spinal cord irradiation injury. *PLoS ONE* 8(2):e57534.

Takizawa T, Anderson CL, Robinson JM (2003) A new method to enhance contrast of ultrathing cryosections for immunoelectron microscopy. *J Histochem Cytochem* 51: 31-39.

Talbott JF, Cao Q, Bertram J, Nkansah M, Benton RL, Lavik E, Whittemore SR (2007) CNTF promotes the survival and differentiation of adult spinal cord-derived oligodendrocyte precursor cells in vitro but fails to promote remyelination in vivo. *Exp Neurol* 204:485-489.

Tashiro A, Zhao C, Gage FH (2006) Retrovirus-mediated single-cell gene knockout technique in adult newborn neurons in vivo. *Nat Protoc* 1(6):3049-3055.

Tripathi R and McTigue DM (2007) Prominent oligodendrocyte genesis along the border of spinal contusion lesions. *Glia* 55: 698-711.

Tripathi R and McTigue DM (2008) Chronically increase ciliary neurotrophic factor and fibroblast growth factor-2 expression after spinal contusion in rats. *J Comp Neurol* 510:129-144.

Tripathi RB, Rivers LE, Young KM, Jamen F, Richardson WD (2010) NG2 glia generate new oligodendrocytes but few astrocytes in a murine experimental autoimmune encephalomyelitis model of demyelinating disease. *J Neurosci* 30:16383-16390.

Vernerey J, Macchi M, Magalon K, Cayre M, Durbec P (2013) Ciliary neurotrophic factor controls progenitor migration during remyelination in the adult rodent brain. *J Neurosci* 33:3240-3250.

Watanabe M, Toyama Y, Nishiyama A (2002) Differentiation of proliferated NG2-positive glial progenitor cells in a remyelinating lesion. *J Neurosci Res* 69:826-836.

Wen S, Li H, Liu J (2009) Dynamic signaling for neural stem cell fate determination. *Cell Adh Migr* 3:107-117.

Yokogami K, Wakisaka S, Avruch J, Reeves SA (2000) Serine phosphorylation and maximal activation of STAT3 during CNTF signaling is mediated by the rapamycin target mTOR. *Curr Biol* 10:47-50.

Zai LJ, Wrathall JR (2005) Cell proliferation and replacement following contusive spinal cord injury. *Glia* 50:247-257.